High lung volume increases stress failure in pulmonary capillaries

ZHENXING FU, MICHAEL L. COSTELLO, KOICHI TSUKIMOTO, RENATO PREDILETTO, ANN R. ELLIOTT, ODILE MATHIEU-COSTELLO, AND JOHN B. WEST
Department of Medicine, University of California, San Diego, La Jolla, California 92093-0623

FU, ZHENXING, MICHAEL L. COSTELLO, KOICHI TSUKIMOTO, RENATO PREDILETTO, ANN R. ELLIOTT, ODILE MATHIEU-COSTELLO, AND JOHN B. WEST. *High lung volume increases stress failure in pulmonary capillaries.* J. Appl. Physiol. 73(1): 123–133, 1992.—We previously showed that when pulmonary capillaries in anesthetized rabbits are exposed to a transmural pressure (Ptm) of ~40 mmHg, stress failure of the walls occurs with disruption of the capillary endothelium, alveolar epithelium, or sometimes all layers. The present study was designed to test whether stress failure occurred more frequently at high than at low lung volumes for the same Ptm. Lungs of anesthetized rabbits were inflated to a transpulmonary pressure of 20 cmH_2O, perfused with autologous blood at 32.5 or 2.5 cmH_2O Ptm, and fixed by intravascular perfusion. Samples were examined by both transmission and scanning electron microscopy. The results were compared with those of a previous study in which the lung was inflated to a transpulmonary pressure of 5 cmH_2O. There was a large increase in the frequency of stress failure of the capillary walls at the higher lung volume. For example, at 32.5 cmH_2O Ptm, the number of endothelial breaks per millimeter cell lining was 7.1 ± 2.2 at the high lung volume compared with 0.7 ± 0.4 at the low lung volume. The corresponding values for epithelium were 8.5 ± 1.6 and 0.9 ± 0.6. Both differences were significant ($P < 0.05$). At 52.5 cmH_2O Ptm, the results for endothelium were 20.7 ± 7.6 (high volume) and 7.1 ± 2.1 (low volume), and the corresponding results for epithelium were 32.8 ± 11.9 and 11.4 ± 3.7. At 32.5 cmH_2O Ptm, the thickness of the blood-gas barrier was greater at the higher lung volume, consistent with the development of more interstitial edema. Ballooning of the epithelium caused by accumulation of edema fluid between the epithelial cell and its basement membrane was seen at 32.5 and 52.5 cmH_2O Ptm. At high lung volume, the breaks tended to be narrower and fewer were oriented perpendicular to the axis of the pulmonary capillaries than at low lung volumes. Transmission and scanning electron microscopy measurements agreed well. Our findings provide a physiological mechanism for other studies showing increased capillary permeability at high states of lung inflation.

blood-gas barrier; lung inflation; capillary endothelium; alveolar epithelium; capillary permeability; pulmonary edema; barotrauma

PREVIOUS STUDIES from this laboratory showed that when pulmonary capillaries in anesthetized rabbits are exposed to a transmural pressure (Ptm) of ~40 mmHg, ultrastructural changes occur in the alveolar wall. These consist of disruption of the capillary endothelium, alveolar epithelium, or sometimes all layers of the wall (18). Because the calculated wall stresses of the capillaries are extremely high under these conditions, we attributed the ultrastructural changes to stress failure (20).

In an effort to understand the various forces acting on the capillary wall, these have been analyzed in some detail (20). The three principal forces are *1*) circumferential or hoop tension in the capillary wall resulting from the Ptm of the capillaries, *2*) surface tension of the alveolar lining layer (because the capillaries bulge into the alveolar spaces at high distending pressures, this surface tension acts to support the wall and reduce the hoop tension), and *3*) longitudinal tension of tissue elements in the alveolar wall associated with lung inflation (depending on the geometry of the capillary in relation to the alveolar wall, increases in this longitudinal tension could increase circumferential tension in the capillary and therefore increase the tendency to stress failure).

In our earlier analysis (20), we concluded that stress failure would probably be more likely at high states of lung inflation on the basis of existing data on capillary morphology at high lung volume. Briefly, these studies (10) showed that the mean width of pulmonary capillaries in rapidly frozen dog lung was reduced at high states of lung inflation for the same capillary Ptm. At high capillary Ptm when the capillaries bulge into the alveolar spaces, this might be explained by the increase in surface tension of the alveolar lining layer as a result of the behavior of surfactant. However, the reduction in mean capillary width was also seen at such low capillary Ptm that they did not bulge into the alveolar spaces. This latter observation appeared to rule out the effects of surface tension in this situation and suggested that lung inflation per se flattened the capillaries, implying that the tension in the capillary wall was raised. However, these predictions clearly need to be tested.

Additional reasons for studying the effects of high lung volume on stress failure of pulmonary capillaries are the observations by other investigators that, at high states of lung inflation, capillary permeability is increased and pulmonary edema tends to occur (4–8, 11, 12, 19). Because stress failure causes damage to the capillary wall, this is a possible explanation for these findings.

Here we report experiments in which capillary Ptm was held constant at 32.5 or 52.5 cmH_2O and lung volume was increased from a transpulmonary pressure of 5 to 20 cmH_2O. The extent of the stress failure in the capillary walls was assessed by morphometric analysis, including the number of endothelial and epithelial breaks per mil-

limeter of endothelial or epithelial cell lining and the size of the endothelial and epithelial breaks. In addition, the appearance of the epithelial breaks was studied by scanning electron microscopy (SEM), because we previously showed that this method of observation gives much additional information (3).

METHODS

In Situ Rabbit Perfused Lung Preparation

We used the in situ vascular perfusion preparation of rabbit lungs described previously (18). Six male rabbits [4.7 ± 0.1 (SD) kg body wt, range 4.5–4.9] were tranquilized and anesthetized by combined intramuscular injections of ketamine (40 mg/kg body wt), acepromazine (0.75 mg/kg), xylazine (4 mg/kg), and atropine (0.4 mg/kg). They were placed supine, heparinized (2,000 U/kg), and rapidly exsanguinated via a cannula inserted into a carotid artery. The trachea was cannulated, and the thorax was rapidly opened. Then two cannulas (Tygon, 3.0 mm diam) were inserted: one through the right ventricle into the main pulmonary artery and the other into the left atrial appendage. Both ventricles were ligated to prevent blood loss into the systemic circulation. After all bubbles were carefully removed, Tygon tubing (9.5 mm diam) was used to connect both cannulas to specific reservoirs (see below), and the rib cage was widely opened to allow the lungs to inflate freely.

The lung was sequentially perfused with the rabbits' own blood, saline-dextran, and then buffered glutaraldehyde as fixative. The reference level for vascular pressures was the middle of the thorax, and the hydrostatic perfusion pressure (inflow) was maintained within ±1 cmH_2O of preset value by adjusting the height of the reservoir connected to the pulmonary artery. The upper level of the solution in the three reservoirs was adjusted at the same height, so that the same pressure was maintained during perfusion with each solution. The outflow reservoir (connected to the pulmonary veins) was set 5 cmH_2O lower than the pulmonary arterial side. Pulmonary arterial and venous pressures were continuously measured during the procedure via two glass manometers connected to the circuit by T tubes inserted close to the inflow and outflow cannulas.

The lungs were first inflated to 25 cmH_2O positive pressure and then deflated to 20 cmH_2O and maintained at that level during the entire procedure. Gil et al. (9) showed that this resulted in a lung volume very close to maximal. The perfusion circuit was first primed with blood from the animal. After 1 min of perfusion with blood, saline-dextran (11.06 g NaCl/l, 350 mosM; 3% T-70 dextran; and 1,000 U heparin/100 ml) was substituted until the outflow appeared clear of blood cells (~3 min). Then fixative (phosphate-buffered 2.5% glutaraldehyde with 3% T-70 dextran; total osmolarity 500 mosM, pH adjusted to 7.4) was perfused for 10 min. As in our previous studies (3, 18, 20), we chose this fixative on the basis of the work of Bachofen et al. (1), who showed that perfusion with isotonic glutaraldehyde solution (total osmolarity 350 mosM) caused extensive edema while a hypertonic solution (510 mosM) yielded good tissue preservation. We also showed that the ultrastructural appearance of lung prepared in this way is normal at a normal capillary pressure of 12.5 cmH_2O (18). During all perfusions, the upper level of the liquids in the reservoirs was adjusted to maintain the preset pressure.

Three animals were randomly assigned to each of the two following groups: 55 and 75 cmH_2O pulmonary arterial pressure. Pulmonary venous pressure was 5 cmH_2O lower than pulmonary arterial pressure in each group, i.e., 50 and 70 cmH_2O, respectively. Therefore capillary hydrostatic pressures were 52.5 and 72.5 ± 2.5 cmH_2O. Because airway pressure was constant (20 cmH_2O), the capillary Ptm were 32.5 and 52.5 ± 2.5 cmH_2O, respectively.

Tissue Sampling

After fixation, the lungs were excised and stored in glutaraldehyde in the refrigerator at 4°C for 1–12 days. One slab, ~0.5 cm thick, was taken perpendicular to the cranial-caudal axis at about one-third the distance from the bottom of either lower lobe in each animal, and one thin vertical slice was obtained from each slab by use of the lung vertical section sampling procedure described by Michel and Cruz-Orive (13). Random numbers were used to cut each vertical slice in a random direction around the vertical axis in each slab. The vertical slices were then cut into smaller blocks (~1.5 × 1.5 × 2.0 mm). They were rinsed overnight in 0.1 M phosphate buffer adjusted to 350 mosM with NaCl (pH 7.4) and processed for transmission electron microscopy (TEM). In each animal at each pressure, tissue blocks from an adjacent vertical slice of the same slab were rinsed in the same buffer as the TEM samples above and then processed for SEM.

Transmission Electron Microscopy

Tissue preparation and morphometry procedures were identical to those used in our previous study (18).

Tissue preparation. Briefly, the samples were postfixed for 2 h in 1% osmium tetroxide in 0.125 M sodium cacodylate buffer adjusted to 350 mosM with NaCl (total osmolarity 400 mosM, pH 7.4). They were dehydrated in increasing concentrations (70–100%) of ethanol, rinsed in propylene oxide, and embedded in Araldite. Five blocks were selected randomly from each vertical slice. Sections (1 μm) were cut from each block with an LKB Ultratome III, stained with 0.1% aqueous solution of toluidine blue, and examined by light microscopy. Ultrathin sections (50–70 nm) were contrasted with uranyl acetate and bismuth subnitrate (16). Micrographs for morphometry were taken on 70-mm films with a Zeiss 10 electron microscope. Micrographs of a carbon-grating replica (E. F. Fullam, Schenectady, NY) were recorded for calibration on each film.

Morphometry. Micrographs were taken by systematic sampling in one ultrathin section from each block. For morphometry, we analyzed five randomly selected blocks, 29–31 micrographs were obtained from each of two blocks, and 12 micrographs from each of three other blocks, yielding a total of 94–98 micrographs from each slab in each animal. A final magnification of ×11,000 was used. Measurements were performed with a Videometric 150 image analyzer (American Innovision) after elec-

tronic positive reversal of the 70-mm negative films. The resolution on the video monitor was not always sufficient to distinguish basement membranes. Therefore a print of each micrograph was available and systematically examined during the measurements. This allowed an unequivocal identification of small endothelial and epithelial disruptions, as well as the presence (or absence) of basement membrane at all sites of rupture.

The following measurements were performed in each field of view. The frequency of disruptions of the blood-gas barrier was quantified as the number of breaks per unit endothelial and epithelial boundary length in the sections. This was achieved by tracing the contour of capillary (inner endothelial) and alveolar (outer epithelial) boundary segments in each field of view and by counting the number of endothelial and epithelial disruptions. The presence or absence of a basement membrane at each disruption site (endothelial or epithelial) and the presence of red blood cells (RBCs) at endothelial break sites) were recorded. The presence and extent of interstitial edema were assessed by measuring the thickness (profile width) of each layer of the blood-gas barrier (endothelium, interstitium, epithelium). One to five sites were systematically sampled in each micrograph (181–248 blood-gas barrier sites measured for thickness in each animal). The measurements were made at right angles to the barrier at random points systematically determined by the image analyzer via electronically generated test lines intersecting the barrier, as described previously (18).

Scanning Electron Microscopy

We used the same SEM tissue preparation and quantitative techniques as in our previous study (3). Briefly, all specimens were conductive stained according to the method of Murakami (14); i.e., they were placed in a solution of 2% arginine, 2% glycine, 2% sodium glutamate, and 2% sucrose (pH 6.2) at 4°C for 16 h; rinsed in distilled water for 30 min; kept in 2% tannic acid (pH 4.0) at room temperature for 24 h; and then rinsed in distilled water. They were then postfixed in 1% osmium tetroxide solution in 0.125 M sodium cacodylate buffer adjusted to 350 mosM with NaCl (total osmolarity 420 mosM, pH 7.4) at room temperature for 4 h. After being rinsed in distilled water, the samples were processed for critical point drying (CPD), i.e., dehydrated in increasing concentrations (70–100%) of ethyl alcohol, transferred to amyl acetate, and dried in a carbon dioxide apparatus (Samdri 790, Tousimis Research).

To assess artifacts during the procedure, all tissues, i.e., four to five tissue blocks from each of two to four samples (from 1 to 2 animals at 32.5 and 52.5 cmH_2O Ptm), were processed in the same CPD run, together with a control taken at a similar sampling site in animals from our previous study that had been exposed to 12.5 cmH_2O Ptm (*animals 2* and *3* in Ref. 18). A third sample from the same slab from one control (*animal 2* in Ref. 18) was also used in our previous SEM study of alveolar epithelial cells at 12.5 cmH_2O Ptm (3).

The dried specimens were mounted on stubs with conductive carbon cement. In each block, the portion of tissue handled with forceps was oriented toward the center of the stub to identify handling artifacts. The tissues were sputter-coated with gold in a Technics Hummer II apparatus and examined with a Cambridge Instruments Stereoscan 360 (20-keV accelerating voltage, 3.0-A filament, and 270-pA probe current).

Quantitative analysis. Every sixth alveolar depression (portion of alveolus extending away from the cut surface of the sample) was chosen by systematic random sampling in one or two blocks selected randomly from each animal (total 5–20 alveoli analyzed in each animal). The Stereoscan's built-in point-to-point system was used to measure the length and midwidth of each disruption and to approximate the planar area of the total alveolar surface examined in each depression. We also recorded the orientation of each break relative to the axis of the capillaries, the distance from the nearest intercellular junctions, and the nature of the disruption (epithelium only or all layers of the air-blood barrier). Depending on the resolution needed to identify the breaks, examination was done at ×2,500–3,500 magnifications. A photograph of each alveolar depression used for quantitative analysis was taken on polaroid film.

Correlation between TEM and SEM measurements. The number of breaks per millimeter epithelial boundary length (measured by TEM) is proportional to the number of breaks per unit alveolar surface area (measured by SEM). In fact, the linear fraction of the breaks (i.e., break number per unit alveolar boundary length × average break length) is equivalent to the areal fraction of breaks (i.e., break number per unit alveolar surface area × break average area). This is the principle of Rosiwal (17). As in our previous study (3), we compared the linear fraction of breaks measured by TEM with their areal fraction measured by SEM to determine whether similar ruptures were analyzed by both methods. This was important because preparation artifacts, in particular cracks, could have occurred in the tissues during SEM preparation and could be confused with stress failure of the alveolar wall.

Statistics

Data were expressed as means ± SE. The SE of the estimates of the number of breaks per unit endothelial and epithelial boundary length (by TEM) was calculated by applying formulas for the SE of ratio (2). The variability between TEM micrographs at the sampling location studied was obtained by pooling the data of the micrographs from two blocks (total 58–61 micrographs). The variability between TEM blocks (for a similar total number of 60 micrographs) was obtained by pooling the data of 12 micrographs within each of five blocks. These were the first 12 micrographs in each of two blocks where 29–31 micrographs were examined and all micrographs from each of three other blocks (see above). The SE of the estimates of break length and blood-gas barrier thickness (by TEM), as well as length and width of breaks (by SEM), indicates the variability between individual measurements.

Group means for different pressures were compared by Student's *t* test. The average break length for the epithe-

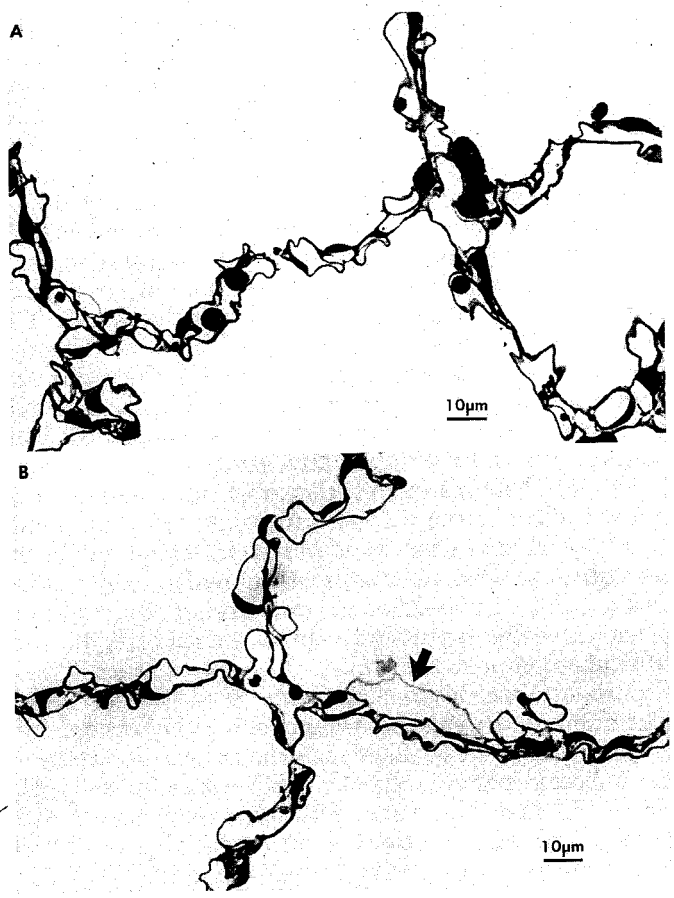

FIG. 1. Light micrographs of portions of lung parenchyma in rabbits perfused at high lung volume, i.e., 20 cmH_2O transpulmonary pressure and 32.5 (*A*) or 52.5 cmH_2O capillary transmural pressure (Ptm) (*B*). Note distension ("ballooning") of epithelial layer by interstitial edema (arrow; see also Fig. 3).

lium and the endothelium, as well as the thickness of the blood-gas barrier compartments at each pressure were compared by paired *t* test. Differences were taken as significant for $P < 0.05$.

RESULTS

Macroscopic Observations

Some frothy pink fluid was seen in the trachea of all six animals. It appeared within 2–5 min of the start of the perfusion at 32.5 cmH_2O Ptm and within 1–3 min at 52.5 cmH_2O Ptm. The fluid was more abundant and of a more reddish color at the higher Ptm, suggesting a larger exudation of RBCs.

Light Microscopy

Figure 1, *A* and *B*, shows the appearance of the lung parenchyma at 32.5 and 52.5 cmH_2O Ptm, respectively. RBCs were found in some capillaries at both pressures despite the 3-min perfusion with saline-dextran. The transpulmonary pressure was 20 cmH_2O in all lungs (see METHODS). As reported by Glazier et al. (10), capillaries were less distended than at a transpulmonary pressure of 5 cmH_2O for the same capillary Ptm (cf. Fig. 1*B* and Fig. 1*C* in Ref. 18). The corner vessels were more distended than many capillaries lining the alveoli, both at 32.5 and 52.5 cmH_2O Ptm (Fig. 1, *A* and *B*). This was expected because corner vessels are believed to be pulled open by the radial traction of the alveolar walls, and they therefore remain open in zone 1 when the capillaries are closed (10). Several capillaries did not appear more distended at 52.5 (Fig. 1*B*) than at 32.5 cmH_2O Ptm (Fig. 1*A*) for the same transpulmonary pressure. This is possibly related to the fact that numerous disruptions of the endothelial wall occurred (see below) and released the high pressure in the capillaries. Substantial distension of the epithelial layer by the edema fluid was seen (Fig. 1*B*).

Transmission Electron Microscopy

General appearance. Disruptions of the blood-gas barrier were found at 32.5 and 52.5 cmH_2O Ptm. Examples of the appearance of the breaks by TEM are shown in Fig. 2, *A–D*. Ruptures were seen on the thick (*B*) and the thin sides (2*C*) of the blood-gas barrier. As reported by Tsukimoto et al. (18), RBCs or platelets were often seen close to or protruding through the openings (Fig. 2, *A–C*). Figure 2*A* shows two RBCs squeezing through an opening and lifting the basement membrane from the endothelium. Sometimes both the endothelium and the epithelium were disrupted, but nevertheless the basement membrane appeared intact (Fig. 2*C*). Figure 2*D* shows an example of multiple ruptures of the epithelial layer, whereas the basement membrane appeared intact. Sometimes the epithelium appeared to break up into small globules ("fragmentation") as in Fig. 3. Widening of the blood-gas barrier by interstitial edema was frequently seen (Fig. 2, *A–D*). Separation of the epithelium from its underlying basement membrane was also frequently seen with thinning and distension of the epithelium (Fig. 3). This appearance ("ballooning") was associated with an accumulation of edema fluid between the epithelial cell and its basement membrane. The same phenomenon was previously observed in rabbit lungs perfused at a transpulmonary pressure of 5 cmH_2O and 52.5 or 72.5 cmH_2O Ptm (see Fig. 2, *C* and *D*, in Ref. 18).

Number and lengths of breaks. The morphometric measurements of the frequency and average length of the endothelial and epithelial breaks (including those with intact and broken basement membrane) for each Ptm are given in Table 1. Figure 4 shows a histogram of the average number of breaks per millimeter endothelial and epithelial boundary length for the present study compared with our previous study where the transpulmonary pressure was 5 cmH_2O (18). For the same Ptm of 32.5 cmH_2O, the number of breaks was significantly larger at a transpulmonary pressure of 20 cmH_2O in the endothelium and epithelium. At 52.5 cmH_2O Ptm, the difference was not significant because of the large intragroup variability (Fig. 4, Table 1). At the high lung volume, i.e., at a transpulmonary pressure of 20 cmH_2O, there were approximately as many endothelial and epithelial breaks at 32.5 as at 52.5 cmH_2O Ptm but lower lung volume (transpulmonary pressure 5 cmH_2O; Fig. 4). Similarly, the number of breaks in endothelium or epithelium at 52.5 cmH_2O Ptm and transpulmonary pressure of 20 cmH_2O (Table 1) was not significantly different from that at 72.5 cmH_2O Ptm and transpulmonary pressure of 5 cmH_2O

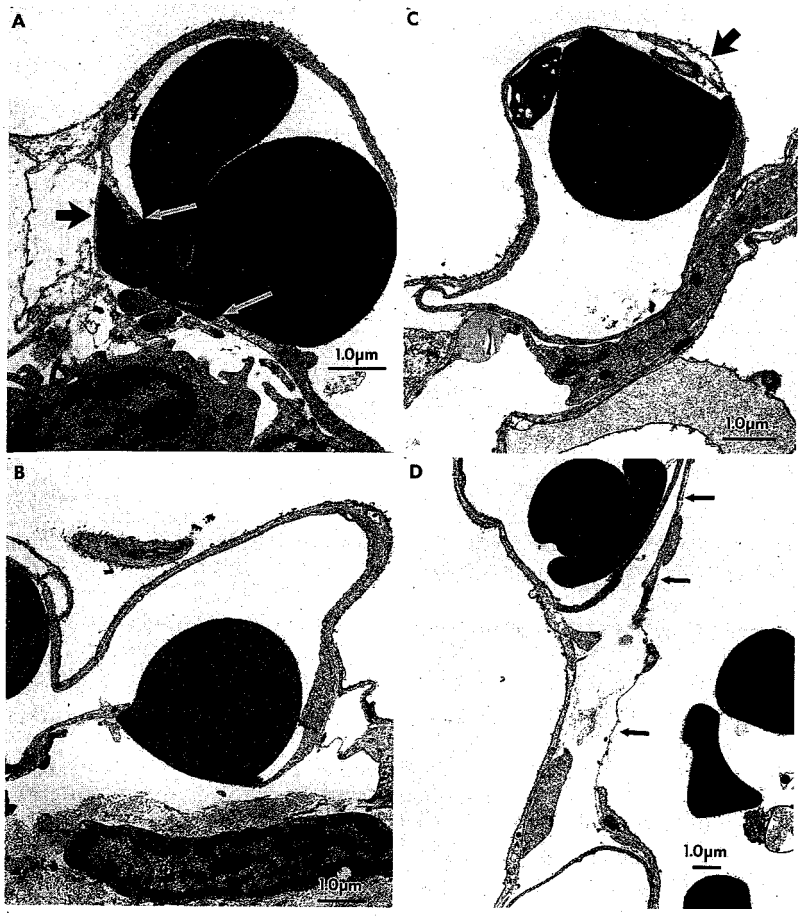

FIG. 2. Transmission electron micrographs showing ultrastructure of blood-gas barrier in rabbit lungs perfused at 20 cmH_2O transpulmonary pressure and 52.5 cmH_2O Ptm. *A*: endothelial discontinuity (arrows) with red blood cells (RBCs) passing through and lifting basement membrane (arrowhead) from endothelium. *B*: endothelial discontinuity on thick side of blood-gas barrier with an RBC protruding into opening. *C*: discontinuities of endothelium and epithelium with intact basement membrane (arrowhead) and adjacent RBC and platelet. *D*: multiple disruptions of epithelial layer (arrows) with intact basement membrane. Note increased interstitial space and RBCs in alveolus.

(data from Ref. 18: 27.8 ± 8.6 and 13.6 ± 1.4 breaks/mm for endothelium and epithelium, respectively).

The difference between the number of breaks at 52.5 and 32.5 cmH_2O Ptm was not significant for endothelium or epithelium, because of the large intragroup variability (Table 1). Data from 2 blocks (total 58–61 micrographs/animal) yielded group means of 22.1 ± 11.9 and 11.3 ± 2.3 endothelial breaks/mm and 26.3 ± 7.0 and 8.1 ± 2.4 epithelial breaks/mm at 52.5 and 32.5 cmH_2O Ptm, respectively. Examining more blocks in each experiment confirmed the large intragroup variability. For both endothelial and epithelial breaks per millimeter, the coefficient of variation between micrographs was not significantly different when micrographs (~60) were taken from five or two blocks (cf. *columns A* and *B* in Table 2). In addition, the coefficient of variation between blocks (Table 2, *column C*) was substantially smaller than that between micrographs in each animal. This indicated that the source of variability in the number of breaks per millimeter was at the level of the micrographs, i.e., individual capillaries rather than regional (between tissue blocks) at the sampling location studied. There was no significant difference in the average length of epithelial or endothelial breaks between 32.5 and 52.5 cmH_2O Ptm or in the average length of epithelial compared with endothelial breaks at each pressure. Again, examining micrographs from two blocks or sampling a similar number of micrographs from a greater area (i.e., sections from 5 tissue blocks) did not result in statistical difference in the data.

FIG. 3. Transmission electron micrograph of blood-gas barrier in rabbit lung perfused at 20 cmH_2O transpulmonary pressure and 52.5 cmH_2O Ptm. Edema fluid accumulation lifted highly stretched and dislocated epithelial layer ("ballooning," solid arrows) from basement membrane (arrowhead). Note epithelial fragmentation (small arrows), endothelial discontinuity (white arrows) with RBCs passing through, and RBCs in interstitium (*) and alveolar space (open arrow).

The breaks were also separated according to whether the basement membrane was intact or broken. At 32.5 cmH_2O Ptm, the percentage of breaks with intact basement membrane was 54 ± 15% for the endothelium and 40 ± 4% for the epithelium. The values at 52.5 cmH_2O Ptm were 61 ± 19% for the endothelium and 54 ± 23% for

TABLE 1. *TEM morphometric measurements of endothelial and epithelial breaks per millimeter and break average length at each Ptm*

Capillary Ptm, cmH_2O	Animal No.	Endothelium		Epithelium	
		Breaks/mm	Break length, μm	Breaks/mm	Break length, μm
		High lung volume			
32.5	*1*	6.3±1.3	0.98±0.22	7.9±2.6	0.97±0.37
32.5	*2*	3.8±2.3	1.03±0.28	6.1±2.0	1.38±0.34
32.5	*3*	11.2±3.3	0.97±0.19	11.4±3.6	0.94±0.16
Mean ± SE†		7.1±2.2*	0.99±0.02	8.5±1.6*	1.10±0.14
52.5	*4*	13.7±2.9	1.95±0.27	54.9±23.2	1.79±0.18
52.5	*5*	35.8±15.2	1.42±0.20	29.2±5.8	1.93±0.31
52.5	*6*	12.6±2.7	0.58±0.08	14.2±2.9	1.08±0.32
Mean ± SE†		20.7±7.6	1.32±0.40	32.8±11.9	1.60±0.26
		Low lung volume			
32.5‡		0.7±0.4	1.05±0.52	0.9±0.6	1.34±0.66
52.5†		7.1±2.1	0.96±0.25	11.4±3.7	1.77±0.36

Values are means ± SE; data are from 5 blocks (total 60 micrographs; SE between blocks) in each animal. TEM, transmission electron microscopy. * Significantly larger ($P < 0.05$) at high than low lung volume at same transmural pressure (Ptm). † $n = 3$. ‡ $n = 6$.

the epithelium. RBCs were found at the site of 23 ± 9% of the endothelial breaks at 32.5 cmH_2O Ptm. The basement membrane was intact in 40 ± 6% of those breaks. At 52.5 cmH_2O Ptm, 45 ± 18% of the endothelial breaks showed RBCs at the site of the rupture, and the basement membrane was intact in 64 ± 14% of them. There was no significant difference in the endothelial or epithelial break lengths with intact and broken basement membranes.

Thickness of the blood-gas barrier. The thickness of each layer of the blood-gas barrier is given in Table 3. At both Ptm values, the interstitium represented almost half the total width of the blood-gas barrier. It was two- and threefold thicker than either the endothelium or the epithelium at 32.5 and 52.5 cmH_2O Ptm, respectively. There was no significant difference in the total thickness of the blood-gas barrier between the two Ptm values. Compared with our previous study, the width of the interstitium (Table 3) was intermediate and significantly greater ($P < 0.05$) than at a similar Ptm of 32.5 cmH_2O but a transpulmonary pressure of 5 cmH_2O. At 52.5 cmH_2O Ptm, the thickness of the interstitium in the present study (Table 3) was not significantly different from that at 52.5 or 72.5 cmH_2O Ptm and transpulmonary pressure of 5 cmH_2O (18).

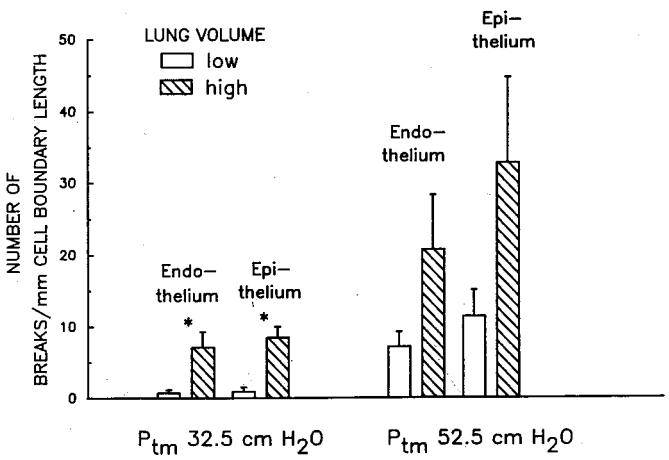

FIG. 4. Histogram of average number of breaks per millimeter endothelium and epithelium at 20 (high lung volume) and 5 cmH_2O (low lung volume; data from Ref. 18) transpulmonary pressure. *Significantly larger ($P < 0.05$) at higher than lower lung volume at the same Ptm.

Scanning Electron Microscopy

General appearance. Figure 5, *A–F,* shows examples of the appearance of the breaks by SEM. Disruptions of the surface of the epithelial cells in the alveolar depressions (see METHODS) were found at 32.5 and 52.5 cmH_2O Ptm. They were either ruptures of all layers of the blood-gas barrier (Fig. 5, *A–C* and *F*) or only disruptions of the epithelial layer (Fig. 5, *E* and *F*). Those breaks that were only ruptures of the epithelial layer were either round (Fig. 5*E*) or elongated and of irregular shape (Fig. 5*F*). The complete ruptures of all layers of the blood-gas barrier were often elongated slits with uneven edges (Fig. 5, *B* and *C*) and irregular shape (Fig. 5*B*). Some breaks showed evidence of retraction of the epithelial layer at the edge of the rupture (Fig. 5*B*). RBCs were often seen under the breaks (Fig. 5, *B* and *C*). Figure 5*D* shows a break close to the boundary of a type II cell. Some breaks were oriented perpendicular to the axis of the pulmonary capillaries (Fig. 5*C*). Others ran mostly parallel (Fig. 5*F*) or at various angles (Fig. 5, *B* and *F*) relative to the axis of the pulmonary capillaries (see below).

Break shape, extent, and number. The number and appearance of the breaks at 32.5 and 52.5 cmH_2O Ptm are given in Table 4. To assess preparation artifacts, tissues were processed in the same CPD run as a control (rabbit lung exposed to 12.5 cmH_2O Ptm and transpulmonary pressure of 5 cmH_2O and similarly prepared; see METHODS). Of 30 alveolar depressions systematically sampled in the controls, five disruptions were found (Table 4). In the animals at 32.5 and 52.5 cmH_2O Ptm, there was considerable variation in the number of breaks between samples (Table 1). The largest number of breaks was found in *animal 5* (52.5 cmH_2O Ptm, Table 4). They were all elongated, and the majority were ruptures of the com-

TABLE 2. *Pool and regional CVs of morphometric estimates of endothelial and epithelial breaks per millimeter at each Ptm*

Capillary Ptm, cmH_2O	Animal No.	Endothelium			Epithelium		
		A	*B*	*C*	*A*	*B*	*C*
				High lung volume			
32.5	*1*	1.55	2.28	0.46	3.12	3.08	0.74
32.5	*2*	2.43	2.61	1.35	1.66	2.14	0.73
32.5	*3*	1.96	2.26	0.66	2.23	2.43	0.71
Mean ± SE*		1.98±0.25	2.38±0.11	0.82±0.27	2.34±0.42	2.55±0.28	0.73±0.01
52.5	*4*	1.58	1.47	0.47	1.83	1.83	0.94
52.5	*5*	1.38	1.63	0.95	1.56	1.41	0.44
52.5	*6*	2.52	2.15	0.48	1.89	2.07	0.46
Mean ± SE*		1.83±0.35	1.75±0.21	0.63±0.16	1.76±0.10	1.77±0.19	0.61±0.16
				Low lung volume†			
32.5‡		6.26±1.32	5.52±1.16	1.99±0.13	5.33±0.79	4.47±0.61	1.96±0.28
52.5*		1.76±0.28	2.51±0.46	0.86±0.12	1.80±0.26	2.75±0.11	0.63±0.02

Values are coefficients of variation (CV = SD/mean). *A*: CV between micrographs (pool, total 58–61) from 2 blocks; *B*: CV between micrographs (pool, total 57–60) from 5 blocks; *C*: CV between 5 blocks (regional). * $n = 3$. † Calculated from Ref. 18. ‡ $n = 6$.

plete blood-gas barrier. Although breaks were found in 9 of 10 alveolar depressions in *animal 5* (Table 4), their number per depression varied largely (range 0–25). In other animals (*1, 3,* and *4*), a few breaks were found in practically every alveolar depression; they were all elongated (*animals 1* and *4*), or about half those breaks were elongated ruptures of the complete blood-gas barrier and half were circular ruptures of only the epithelium. Only two breaks were found in the 20 alveolar depressions sampled in *animal 2* (Table 4).

Break orientation. Of a total of 205 elongated breaks, 48% were oriented perpendicular to the axis of the pulmonary capillaries, 31% were parallel, and 20% were composed of several segments with multiple orientations (Fig. 5, *B* and *F*; Table 5). This contrasts with our recent SEM study of rabbit lungs exposed to similar Ptm values but lower lung volume, i.e., a transpulmonary pressure of 5 cmH_2O. In that study, of a total of 403 elongated breaks examined at 12.5, 32.5, 52.5, and 72.5 cmH_2O Ptm, 68% were oriented perpendicular and 26% were parallel, and only two breaks were oriented obliquely to the capillary axis. None showed multiple segments with different orientations (3).

Break dimensions. The average length of the complete ruptures of the blood-gas barrier was 5.1 ± 0.9 μm (n = 31) at 32.5 cmH_2O Ptm and 7.4 ± 0.5 μm (n = 166) at 52.5 cmH_2O Ptm. These values were not significantly different from those in similar breaks, i.e., elongated ruptures of the whole blood gas barrier at lower lung volume (5 cmH_2O transpulmonary pressure) and a similar Ptm of 32.5 or 52.5 cmH_2O (3). The average widths (1 measurement, taken midlength in each break) were 0.51 ± 0.05 and 0.90 ± 0.09 μm at high lung volume and 32.5 and 52.5 cmH_2O Ptm, respectively. These values were significantly smaller than those of similar breaks at lower lung volume and 32.5, 52.5, or 72.5 cmH_2O Ptm (3). Thus, at the higher lung volume, the breaks were of similar length but were narrower than at lower lung volume for the same capillary Ptm. The dimensions of the circular ruptures of only the epithelium (most of the few circular breaks at 32.5 and 52.5 cmH_2O Ptm) were not significantly different from those of similar breaks at 32.5, 52.5,

TABLE 3. *Blood-gas barrier dimensions at each capillary Ptm*

Capillary Ptm, cmH_2O	Animal No.	Thickness, μm			
		Endothelium	Interstitium	Epithelium	Total
			High lung volume		
32.5	*1*	0.17±0.01	0.35±0.04	0.18±0.00	0.71±0.04
32.5	*2*	0.20±0.01	0.50±0.06	0.20±0.01	0.90±0.06
32.5	*3*	0.22±0.01	0.62±0.06	0.22±0.01	1.07±0.06
Mean ± SE*		0.20±0.01‡	0.49±0.08‡§	0.20±0.01‡	0.89±0.10§
52.5	*4*	0.19±0.01	0.68±0.08	0.21±0.01	1.08±0.08
52.5	*5*	0.17±0.01	0.85±0.10	0.20±0.01	1.23±0.10
52.5	*6*	0.18±0.01	0.51±0.05	0.20±0.01	0.88±0.05
Mean ± SE*		0.18±0.01‡	0.68±0.10‡	0.20±0.00‡	1.06±0.10
			Low lung volume		
32.5†		0.19±0.01	0.17±0.00§	0.19±0.01	0.55±0.01§
52.5*		0.22±0.01‡	0.70±0.04‡	0.25±0.01‡	1.17±0.06

Values are means ± SE. * $n = 3$. † $n = 6$. ‡ Interstitium significantly larger than endothelium or epithelium at same lung volume and Ptm ($P < 0.05$). § Larger at high than at low lung volume ($P < 0.05$).

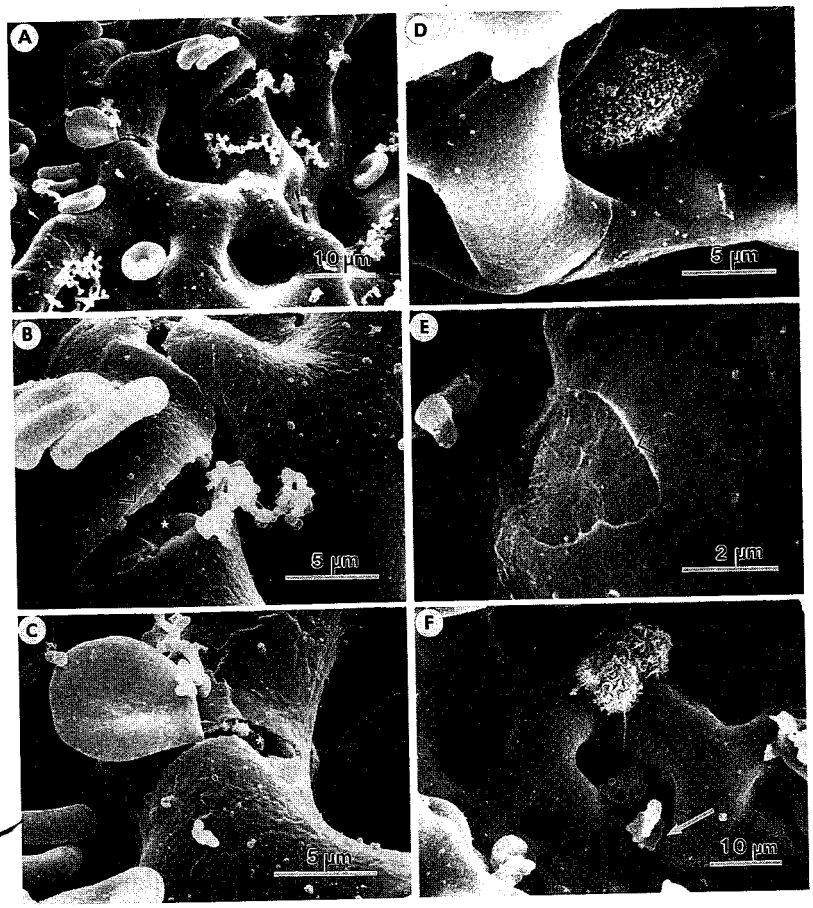

FIG. 5. Scanning electron micrographs showing examples of disruptions of blood-gas barrier in rabbit lungs perfused at 20 cmH_2O transpulmonary pressure and 52.5 cmH_2O Ptm. *A*: adjacent capillaries with complete ruptures of blood-gas barrier (solid arrows) at various angles relative to capillary axis (higher magnifications are shown in *B* and *C*). Note abundance of RBCs and proteinaceous material on alveolar surface. *B*: higher magnification of *A* showing retraction of epithelial layer on edge of break (open arrows) and RBCs in opening (*). *C*: complete rupture of blood-gas barrier with an RBC protruding into opening and others underneath (*). *D*: slits of blood-gas barrier (solid arrows) ~0.6 μm from boundary of type II cell (arrowhead). *E*: round rupture involving only epithelial layer (open arrow). *F*: capillaries showing disruption of only the epithelium (open arrow), a flap of endothelium (white arrow) partly covering 1 break, and a rupture composed of several segments with multiple orientations (solid arrow).

or 72.5 cmH_2O Ptm and a transpulmonary pressure of 5 cmH_2O (3).

Distance between breaks and the nearest intercellular junction. None of the total of 240 breaks (Table 4) occurred in the vicinity of an alveolar epithelial intercellular junction. This is in keeping with our previous finding of only 25 of 443 breaks within 10 μm of a junction at low lung volume (3). It is possible that intercellular junctions were less visible in this study because of the high lung inflation. Also the visualization of the junctions de-

TABLE 4. *Break number and appearance*

	No. of Alveoli		Total Alveolar Surface, μm^2	No. of Breaks						
					Elongated			Circular		
	Total	Without break		Total	Epithelium rupture only	Whole blood-gas barrier	Total examined	Epithelium rupture only	Whole blood-gas barrier	Total examined
					*12.5 cmH_2O Ptm**					
Control 1	15	11	18,000	5	0	5	5	0	0	0
Control 2	15	15	24,000	0	0	0	0	0	0	0
Total	30	26	42,000	5	0	0	5	0	0	0
					32.5 cmH_2O Ptm					
Animal 1	5	1	5,000	15	0	15	15	0	0	0
Animal 2	20	19	26,000	2	0	2	2	0	0	0
Animal 3	17	2	24,000	27	1	14	15	9	3	12
Total	42	22	55,000	44	1	31	32	9	3	12
					52.5 cmH_2O Ptm					
Animal 4	6	1	11,000	32	0	32	32	0	0	0
Animal 5	10	1	28,000	112	3	109	112	0	0	0
Animal 6	14	6	21,000	47	3	25	28	18	1	19
Total	30	7	60,000	191	6	166	172	18	1	19
Total (all pressures)				240	7	202	209	27	4	31

Controls 1 and *2* are tisues from *animals 2* and *3*, respectively, in Ref. 18. * Lung was fixed at transpulmonary pressure of 5 cmH_2O.

TABLE 5. *Break orientation (elongated breaks)*

	No. of Breaks				
	Total examined*	Orientation relative to capillary axis			
		Perpendicular	Parallel	Multiple	Oblique
		12.5 cmH$_2$O Ptm			
Control 1	5	2	3	0	0
		32.5 cmH$_2$O Ptm			
Animal 1	15	9	2	3	0
Animal 2	2	0	0	1	0
Animal 3	15	5	10	0	0
Total	32	14	12	4	0
		52.5 cmH$_2$O Ptm			
Animal 4	32	19	11	2	0
Animal 5	111	51	26	33	0
Animal 6	25	12	10	3	0
Total	168	82	47	38	0
Total	205	98	63	40	0

* Orientation of remainder was not identified.

pended on the angle between the alveolar surface and the electron beam. For example, Fig. 5*D* shows a break in an alveolar epithelial type I cell ~0.6 μm away from the edge of a type II cell. The junction between the two cells is not visible because the beam is orientated at a right angle to the surface of the sample (see also Ref. 3). It is interesting to note that the break occurred very close to the junction but not at the junction itself. In our previous study, we found almost no breaks at intercellular junctions between type I epithelial cells, although some were seen within 1 μm of the junctions (3).

Comparison of SEM and TEM Measurements

SEM. The shape of the single elongated breaks was intermediate between a diamond and a rectangle. As in our previous study (3), we approximated the average area of the elongated breaks by multiplying their width by three-fourths of their length (area of diamond = width × ½ length; area of rectangle = width × length). The average area of the multiple breaks was approximated by multiplying the total length of the segments by their average width. In *animal 5,* where the largest number of breaks was found by SEM, the average area of elongated ruptures of all layers of the blood-gas barrier was 3.08 ± 0.51 μm^2 (single) and 12.6 ± 2.2 μm^2 (multiple breaks), and the average area of ruptures of only the epithelium was 3.0 ± 0.9 μm^2. Accounting for the number of breaks of each type (Tables 4 and 5) yielded a total break area of 651 ± 296 μm^2 in that sample. Because we examined a total alveolar surface area of ~28,000 μm^2 (Table 4), the areal fraction of the breaks (i.e., total break area/alveolar surface area) was 0.023 ± 0.011.

TEM. Multiplying the average length of the epithelial breaks by their number per unit alveolar boundary length (Table 1) gives a linear fraction of the breaks (i.e., total break length/unit boundary length of alveolar surface) of 0.056 ± 0.014 in *animal 5.*

As previously described (3), we expect the areal fraction of the breaks measured by SEM and their linear fraction calculated from measurements by TEM to be equivalent measurements (principle of Rosiwal, 1898). The measurements by SEM and TEM were not significantly different, indicating that similar ruptures were analyzed by scanning and transmission electron microscopy.

DISCUSSION

Lung Inflation Increases the Frequency of Stress Failure of Pulmonary Capillaries

The main finding from the present study is that when the capillaries are exposed to a high Ptm, a high state of lung inflation results in a much greater frequency of stress failure than a low lung volume (Table 1, Fig. 4). For example, at a capillary (Ptm) of 32.5 cmH$_2$O, increasing lung volume from a transpulmonary pressure of 5 to 20 cmH$_2$O resulted in an increase in the number of breaks in the capillary endothelium from 0.7 ± 0.4 to 7.1 ± 2.2 mm. The corresponding values for epithelium were 0.9 ± 0.6 and 8.5 ± 1.6. Both differences are significant at the 5% level.

These results are particularly striking because a capillary Ptm of 32.5 cmH$_2$O is below the "critical" pressure for some lungs. For example, in the previous study by Tsukimoto et al. (18), three of the six lungs studied at a capillary Ptm of 32.5 cmH$_2$O (5 cmH$_2$O transpulmonary pressure) showed no endothelial breaks, and two lungs showed no epithelial breaks. Thus this capillary pressure is too low to produce stress failure in many lungs at a normal volume but produces obvious stress failure at high lung volumes.

When the capillary Ptm was raised to 52.5 cmH$_2$O, many breaks were seen at the low lung volume but the number was much increased at the high lung volume. For the endothelium the values were 7.1 ± 2.1 at the low volume and 20.7 ± 7.6 at the high volume; for the epithelium the corresponding values were 11.4 ± 3.7 and 32.8 ± 11.9. These differences were not significantly different at the 5% level because of the large intragroup variability (see below). However, they suggest a trend toward more stress failure at higher states of lung inflation.

Our demonstration that high lung volume increases the likelihood of stress failure in the walls of the capillaries is consistent with previous physiological data on the dimensions of pulmonary capillaries at high states of lung inflation. For example, Glazier et al. (10) clearly showed that the mean width of the capillaries was greatly reduced when the transpulmonary pressure was increased from 10 to 25 cmH$_2$O (see Fig. 8 of Ref. 10). In these studies, the lungs were in zone 3 condition (venous pressure exceeding alveolar pressure) and the arteriovenous pressure difference was only 4 cmH$_2$O. Therefore the abscissa labeled "distance down zone 3 (cm)" in their Fig. 8 is very nearly equivalent to capillary Ptm in cmH$_2$O.

As shown in Fig. 8 of Ref. 10, increasing the transpulmonary pressure from 10 to 25 cmH$_2$O reduced the mean width of the capillaries from ~5.5 to 4.5 μm at a capillary Ptm of 35 cmH$_2$O. At a lower capillary Ptm of ~2 cmH$_2$O, the results were even more striking in that increasing lung volume from a transpulmonary pressure of 10 to 25 cmH$_2$O reduced the mean width of the capillaries

from ~3.5 to <2 μm. The mean width of the capillary in that study was obtained by measuring the distance across the capillary at right angles to the alveolar wall at equal intervals along the alveolar wall where a capillary was encountered. It therefore included measurements across chord lengths that were much less than the maximum diameter and should not be construed as indicating the maximum diameter of the capillaries.

There are two reasons why increasing lung inflation can be expected to reduce capillary diameter. One is that the surface tension of the alveolar lining layer increases at high lung volumes, and insofar as the capillaries protrude into the alveolar spaces, they will be flattened as the surface tension increases (20). This mechanism could partly explain the reduction in capillary width seen by Glazier et al. (10) at a capillary Ptm of 35 cmH_2O. However, as indicated above, an even more striking reduction in width (in percentage terms) was seen at a capillary Ptm of ~2 cmH_2O. At this very low pressure, the capillaries do not bulge into the alveolar spaces (10), and therefore the marked narrowing of the capillaries cannot be ascribed to surface tension effects.

The second mechanism available to reduce the width of capillaries at high lung volumes is the longitudinal tension in the alveolar wall, which increases with lung inflation. As previously discussed (20), the extent to which this increase in alveolar wall tension is transmitted to the capillaries depends on the geometry of the capillary in the alveolar wall (see Fig. 6 of Ref. 20). If the capillary is located symmetrically within the alveolar wall and the blood-gas barrier is identical on both sides, we can expect that the tensile force carried by the tissue elements of the alveolar wall will be equally shared by the two sides of the capillary. If on the other hand, the capillary is very asymmetrically located in the alveolar wall and the whole of the tension of the tissue elements in the wall is transmitted through the thick side, which contains fibers of type I and type III collagen, little if any increase in hoop tension of the capillary might result. However, the results of Glazier et al. (10) show that, even at very low capillary Ptm values, marked narrowing of the capillaries occurs with lung inflation, strongly suggest that tension within the alveolar wall is partly transmitted to the capillaries, resulting in an increase in their hoop wall tension; this is entirely consistent with our finding that the likelihood of stress failure increases.

The results presented here are also consistent with other studies indicating that capillary microvascular permeability is increased at high states of lung inflation. For example, Parker et al. (15) measured the filtration coefficient and the isogravimetric capillary pressure in isolated blood-perfused dog lungs and showed that the filtration coefficient was increased and the isogravimetric capillary pressure was reduced when the peak airway inflating pressure exceeded ~40 cmH_2O. The fact that a higher airway pressure was required for these dog lungs compared with our rabbit lungs is consistent with recent measurements in our laboratory suggesting that the "critical" pressure required for stress failure is higher in the dog than in the rabbit. Other investigators have also reported that lung inflation to high levels increases pulmonary capillary permeability or results in pulmonary edema (4, 6–8, 11, 12, 19; for a recent review, see Ref. 5).

An interesting feature of the results shown in Fig. 4 is that the increase in number of breaks per millimeter is approximately the same for nearly the same rise in transpulmonary pressure, on the one hand, and capillary Ptm, on the other. Thus, raising the transpulmonary pressure from 5 to 20 cmH_2O (difference 15 cmH_2O) increased the number of endothelial breaks from 0.7 to 7.1. On the other hand, when the transpulmonary pressure was kept at 5 cmH_2O and instead the capillary Ptm was raised from 32.5 to 52.5 cmH_2O (difference 20 cmH_2O), the number of endothelial breaks rose from 0.7 to 7.1. The values for epithelial breaks per millimeter lining showed the same pattern. An increase in transpulmonary pressure from 5 to 20 cmH_2O at a capillary Ptm of 32.5 cmH_2O increased the number of epithelial breaks from 0.9 to 8.5. Compare this with the increase in number of epithelial breaks when the capillary Ptm was raised by 20 cmH_2O; this produced an increase to 11.4.

The above results suggest that, under the conditions studied, an increase in capillary Ptm and transpulmonary pressure are approximately equivalent in terms of their effect on capillary wall stress. This presumably means that much of the longitudinal tension in the alveolar wall resulting from lung inflation is directly transmitted to the capillary walls.

Orientation and Dimensions of Breaks

In a previous study of SEM appearances of epithelial cell breaks at a normal lung volume (5 cmH_2O transpulmonary pressure), we found that the majority (68%) of the elongated breaks were oriented perpendicular to the axis of the pulmonary capillary. This was initially surprising, because when stress failure is caused by a very high hoop stress, for example, in a garden hose that bursts, the break tends to occur along the length of the hose because the hoop stress exceeds the stress in the longitudinal direction. We attributed the finding that the breaks occurred across the capillary to the fact that the surface tension of the alveolar lining layer played an important protective role in preventing stress failure, and that the main support from the surface tension is in the circumferential direction of the capillary because of its shape (see Fig. 6 of Ref. 3).

However, an interesting finding in the present study was that a smaller percentage (48 vs. 68%) of elongated breaks was oriented perpendicular to the axis of the capillary. A possible explanation is that at high states of lung inflation the wall stress of the capillaries is increased in all directions because of uniform stretching of the alveolar wall, and, therefore, the support offered by the surface tension of the alveolar lining layer does not dominate, as it does at low lung volumes. The more uniform stretching of the alveolar wall would also be consistent with the fact that the epithelial breaks often radiated in all directions. Breaks with multiple segments in different orientation were not seen at low lung volume (3).

Another interesting finding in the present study was that the breaks at high volumes tended to be thinner

than those at low lung volumes. Possibly the breaks are distorted by the high state of tension in the alveolar wall.

Variability in the Number of Breaks Within and Between Animals

In this and our previous studies of stress failure, considerable variability exists in the number of breaks both within and between animals. For example, as regards variability within a given lung, in *animal 5* (see RESULTS), although breaks were found in 9 of 10 alveolar depressions (Table 3), their number per depression varied from 0 to 25. Also the intragroup variability in the number of breaks per millimeter of endothelium and epithelium at each Ptm remained when sampling was spread over a wider volume of tissue (i.e., micrographs were taken from 5 randomly chosen tissue blocks instead of 2) at the sampling location studied in each animal. The source of variability in stress failure was at the level of micrographs, i.e., individual capillaries, rather than between tissue blocks (Table 2).

A great variability is to be expected when the end point is failure of a structure, as is the case here. The stress at which failure occurs (ultimate stress) depends on the weakest link in the chain, and in a structure so heterogeneous as the wall of the pulmonary capillary, it is inevitable that there will be large variations both within a given lung and between animals. For this reason it is much easier to show a trend than a significant change in the number of breaks. For example, Fig. 4 shows a larger number of endothelial and epithelial breaks at the high as opposed to the low lung volume for a capillary Ptm of 52.5 cmH_2O. However, the differences are not significant because of the large intragroup variability. Nevertheless the fact that the trend is consistent with that for a capillary Ptm of 32.5 cmH_2O, where the differences were significant, strongly suggests that the phenomenon also exists at the higher capillary Ptm.

We are indebted to Leslie Hempleman, Carlita Durand, Richard Logemann, and Jeff Struthers for technical assistance.

The study was supported by National Heart, Lung, and Blood Institute Program Project Grant HL-17331-16.

Address for reprint requests: J. B. West, Dept. of Medicine 0623, University of California, San Diego, La Jolla, CA 92093-0623.

Received 11 June 1991; accepted in final form 30 January 1992.

REFERENCES

1. BACHOFEN, H., A. AMMANN, D. WANGENSTEEN, AND E. R. WEIBEL. Perfusion fixation of lungs for structure-function analysis: credits and limitation. *J. Appl. Physiol.* 53: 528–533, 1982.
2. COCHRAN, W. G. *Sampling Techniques* (3rd ed.). New York: Wiley, 1977.
3. COSTELLO, M. L., O. MATHIEU-COSTELLO, AND J. B. WEST. Stress failure of alveolar epithelial cells studied by scanning electron microscopy. *Am. Rev. Respir. Dis.* In press.
4. DREYFUSS, D., G. BASSET, P. SOLER, AND G. SAUMON. Intermittent positive-pressure hyperventilation with high inflation pressures produces pulmonary microvascular injury in rats. *Am. Rev. Respir. Dis.* 132: 880–884, 1985.
5. DREYFUSS, D., AND G. SAUMON. Lung overinflation. Physiologic and anatomical alterations leading to pulmonary edema. In: *Adult Respiratory Distress Syndrome,* edited by W. M. Zapol and F. Lemaire. New York: Dekker, 1991, p. 433–449. (Lung Biol. Health Dis. Ser.)
6. EGAN, E. A. Response of alveolar epithelial solute permeability to changes in lung inflation. *J. Appl. Physiol.* 49: 1032–1036, 1980.
7. EGAN, E. A. Lung inflation, lung solute permeability, and alveolar edema. *J. Appl. Physiol.* 53: 121–125, 1982.
8. EGAN, E. A., R. M. NELSON, AND R. E. OLVER. Lung inflation and alveolar permeability to non-electrolytes in the adult sheep in vivo. *J. Physiol. Lond.* 260: 409–424, 1976.
9. GIL, J., H. BACHOFEN, P. GEHR, AND E. R. WEIBEL. Alveolar volume-surface area relation in air- and saline-filled lungs fixed by vascular perfusion. *J. Appl. Physiol.* 47: 990–1001, 1979.
10. GLAZIER, J. B., J. M. B. HUGHES, J. E. MALONEY, AND J. B. WEST. Measurements of capillary dimensions and blood volume in rapidly frozen lungs. *J. Appl. Physiol.* 26: 65–76, 1969.
11. JOHN, E., M. MCDEVITT, W. WILBORN, AND G. CASSADY. Ultrastructure of the lung after ventilation. *Br. J. Exp. Pathol.* 63: 401–407, 1982.
12. KIM, K.-J., AND E. D. CRANDALL. Effects of lung inflation on alveolar epithelial solute and water transport properties. *J. Appl. Physiol.* 52: 1498–1505, 1982.
13. MICHEL, R. P., AND L. M. CRUZ-ORIVE. Application of the Cavalieri principle and vertical sections method to lung: estimation of volume and pleural surface area. *J. Microsc.* 150: 117–136, 1988.
14. MURAKAMI, T. A revised tannin-osmium method for non-coated scanning electron microscope specimens. *Arch. Histol. Jpn.* 36: 189–193, 1974.
15. PARKER, J. C., M. I. TOWNSLEY, B. RIPPE, A. E. TAYLOR, AND J. THIGPEN. Increased microvascular permeability in dog lungs due to high peak airway pressures. *J. Appl. Physiol.* 57: 1809–1816, 1984.
16. RIVA, A. A simple and rapid staining method for enhancing the contrast of tissue previously treated with uranyl acetate. *J. Microsc. Paris* 19: 105–108, 1974.
17. ROSIWAL, A. Ueber geometrische Gesteinsanalysen. *Verh. K. K. Geol. Reichsanst. Wien.* 6: 143, 1898.
18. TSUKIMOTO, K., O. MATHIEU-COSTELLO, R. PREDILETTO, A. R. ELLIOTT, AND J. B. WEST. Ultrastructural appearances of pulmonary capillaries at high transmural pressures. *J. Appl. Physiol.* 71: 573–582, 1991.
19. WEBB, H. H., AND D. F. TIERNEY. Experimental pulmonary edema due to intermittent positive pressure ventilation with high inflation pressures. Protection by positive end-expiratory pressure. *Am. Rev. Respir. Dis.* 110: 556–565, 1974.
20. WEST, J. B., K. TSUKIMOTO, O. MATHIEU-COSTELLO, AND R. PREDILETTO. Stress failure in pulmonary capillaries. *J. Appl. Physiol.* 70: 1731–1742, 1991.